Dynamics and Shocks from Hα Emission of Nearby Galaxy Mergers

S. Alireza Mortazavi,[1⋆] Jennifer M. Lotz,[2]
[1] *Department of Physics and Astronomy, Johns Hopkins University, 3400 N Charles St., Baltimore MD, USA*
[2] *Space Telescope Science Institute, 3700 San Martin Dr., Baltimore MD, USA*

Accepted XXX. Received YYY; in original form ZZZ

ABSTRACT

We examine the dynamical properties of interacting galaxies and the properties of shocked gas produced as a result of the interaction. We observed 22 galaxy mergers using the SparsePak IFU at Kitt Peak National Observatory (KPNO). The goal of the observations was to obtain the Hα velocity maps over the entire luminous parts of the galaxies including the faint tidal tails, and to find extended shocks and outflows. Our sample consists of major and minor galaxy mergers with mass ratios $1 < \mu < 8$. We fit multiple kinematic components to the Hα and [N II] emission lines, develop an MCMC code to robustly estimate the error of fit parameters, and use the F-test to determine the best number of kinematic components for each fiber. We use [N II]/Hα and velocity dispersion of components to separate star-forming (HII) regions from shocks. We use the kinematics of the Hα emission from HII regions and an automated modeling method to put the first ever constraints on the encounter parameters of one of the observed systems. Besides, we estimate the fraction of shocked Hα emission, $f_{shocked}$, and examine the spatial distribution of shocks. We find that close galaxy pairs have, on average, a higher shock fraction than wide pairs, and coalesced mergers have the highest average $f_{shocked}$. In addition, galaxy pairs with more equal mass ratio tend to have a higher $f_{shocked}$. Combining the dynamical models from the literature and this work, we inspect trends between $f_{shocked}$ and dynamical encounter parameters. Our findings are generally consistent with shocks being produced either by direct collision of the ISM or by the chain of events provoked by the tidal impulse during the first passage.

Key words: galaxies: interactions – galaxies: kinematics and dynamics – galaxies: peculiar

1 INTRODUCTION

Sanders & Mirabel 1996; Mihos & Hernquist 1996; de Grijs et al. 2003; Cox et al. 2008). In case of certain encounter

- На ранней стадии мержинга: радиальные движения к центру, столкновения газовых потоков, ударные волны.
- Позднее: прямые столкновения газа двух дисков.
- И то, и другое, стимулирует звездообразование, и ответственно за эмиссионный спектр галактики.
- Существенная часть потока На может быть связана с ударным возбуждением.

Цель: кинематические особенности галактик и межзвёздного газа при мержинге.

- We observed 22 galaxy mergers using the SparsePak IFU at Kitt Peak National Observatory (KPNO). The goal of the observations was to obtain the H velocity maps over the entire luminous parts of the galaxies including the faint tidal tails, and to find extended shocks and outows.
- Our sample consists of major and minor galaxy mergers with mass ratios $1 < \mu < 8$.
- 82 фибера 5” в диаметре.

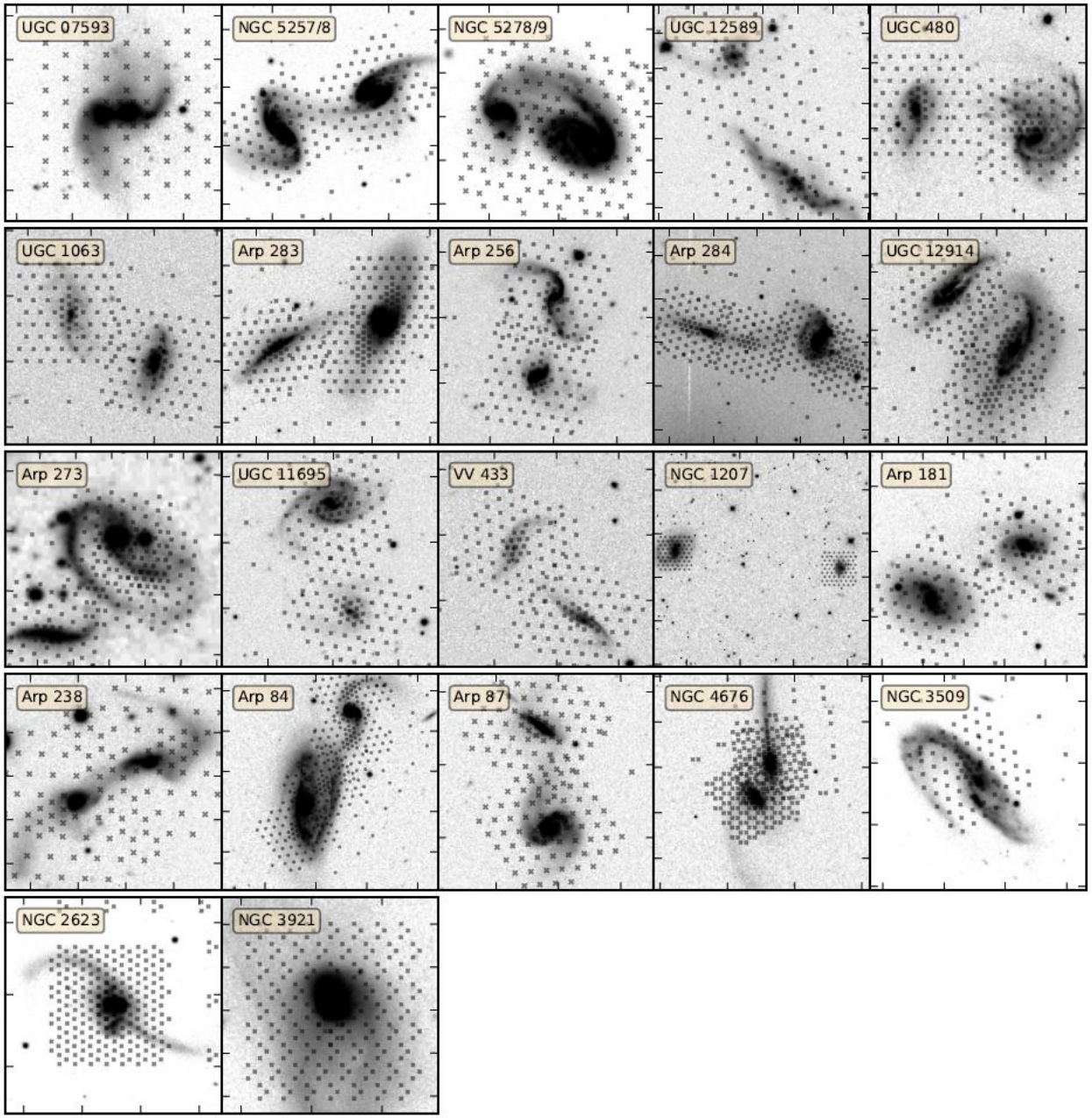
UGC 07593
NGC 5257/8
NGC 5278/9
UGC 12589
UGC 480
UGC 1063
Arp 283
Arp 256
Arp 284
UGC 12914
Arp 273
UGC 11695
VV 433
NGC 1207
Arp 181
Arp 238
Arp 84
Arp 87
NGC 4676
NGC 3509
NGC 2623
NGC 3921

system name	RA	DEC	observation date	redshift
UGC 12914	0.4171	23.4898	Oct 2012	0.0146
Arp 256	4.7104	-10.3693	Oct 2012	0.0272
VV 433	9.8322	13.1064	Oct 2012	0.0353
UGC 480	11.6472	36.3286	Oct 2012	0.0374
UGC 1063	22.2881	11.1360	Oct 2012	0.0193
Arp 273	35.3778	39.3660	Oct 2012	0.0251
NGC 1207	47.0034	38.3769	Oct 2012	0.0160
NGC 2623	129.6001	25.7545	Mar 2008	0.0185
Arp 283	139.3624	41.9970	Oct 2012	0.0060
Arp 181	157.1193	79.8182	May 2013	0.0326
NGC 3509	166.0981	4.8286	Mar 2008	0.0257
Arp 87	175.1850	22.4379	May 2013	0.0237
NGC 3921	177.7786	55.0788	Mar 2008	0.0197
UGC 07593	187.0612	44.4532	Apr 2012	0.0230
NGC 4676	191.5443	30.7271	Mar 2008	0.0220
Arp 238	198.8870	62.1269	May 2013	0.0308
NGC 5257/8	204.9805	0.8354	Apr 2012	0.0227
NGC 5278/9	205.4237	55.6722	Apr 2012	0.0252
Arp 84	209.6492	37.4391	May 2013	0.0116
UGC 11695	318.0418	-1.4857	Oct 2012	0.0323
UGC 12589	351.2615	0.0096	Oct 2012	0.0338
Arp 284	354.0750	2.1557	Oct 2012	0.0093

Our observations were carried out in the wavelength range 6050-7000A and did not include Hb and [O III] emission lines, so we can not use the BPT diagnostic diagrams to separate the emission lines. On the other hand, our SparsePak observations have a relatively high velocity resolution of 30 km/s making it possible to use the width of emission lines to separate star formation and shocks.

- Monreal-Ibero et al. ApJ,637, 138 (2006) showed that in a shock-heated gas, the velocity dispersion of emission lines is correlated with low-ionization line ratios particularly with [O I]/Ha and [N II]/Ha.
- Ударное возбуждение: (критерий Rich et al, 2015 : >90 км/с).
- Более продвинутый подход: Mortazavi et al. MNRAS 474,3423 (2018),

Области 2 и 3 –
Ударное возбуждение

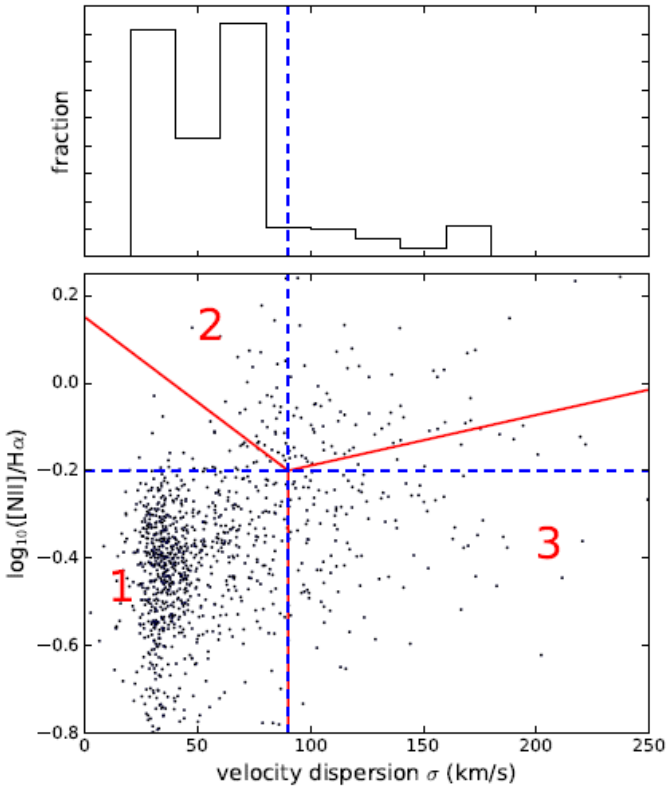

Figure 4. Plot of $\log_{10}$([N II]/Hα) vs. velocity dispersion for all 956 components in all galaxies in our sample. These are the components with S/N>3 in fibers with Hα EW > 7Å. The concentration of points around 30 km/s is probably due to velocity resolution of our observations. Red lines are taken from Mortazavi et al. (2018) and show how we determine the source of ionization. The blue dashed vertical (horizontal) line shows the limit of σ = 90 km/s ($\log_{10}$([N II]/Hα)=-0.2). In this work, we take Group 1 as star-forming regions, and Groups 2 and 3 as shocks. The panel on top shows the Hα flux weighted histogram of all components. Similar to some systems in Rich et al. (2011) and Rich et al. (2015) we find a significant bumps in the Hα flux at high velocity dispersion (~ 160 km/s).

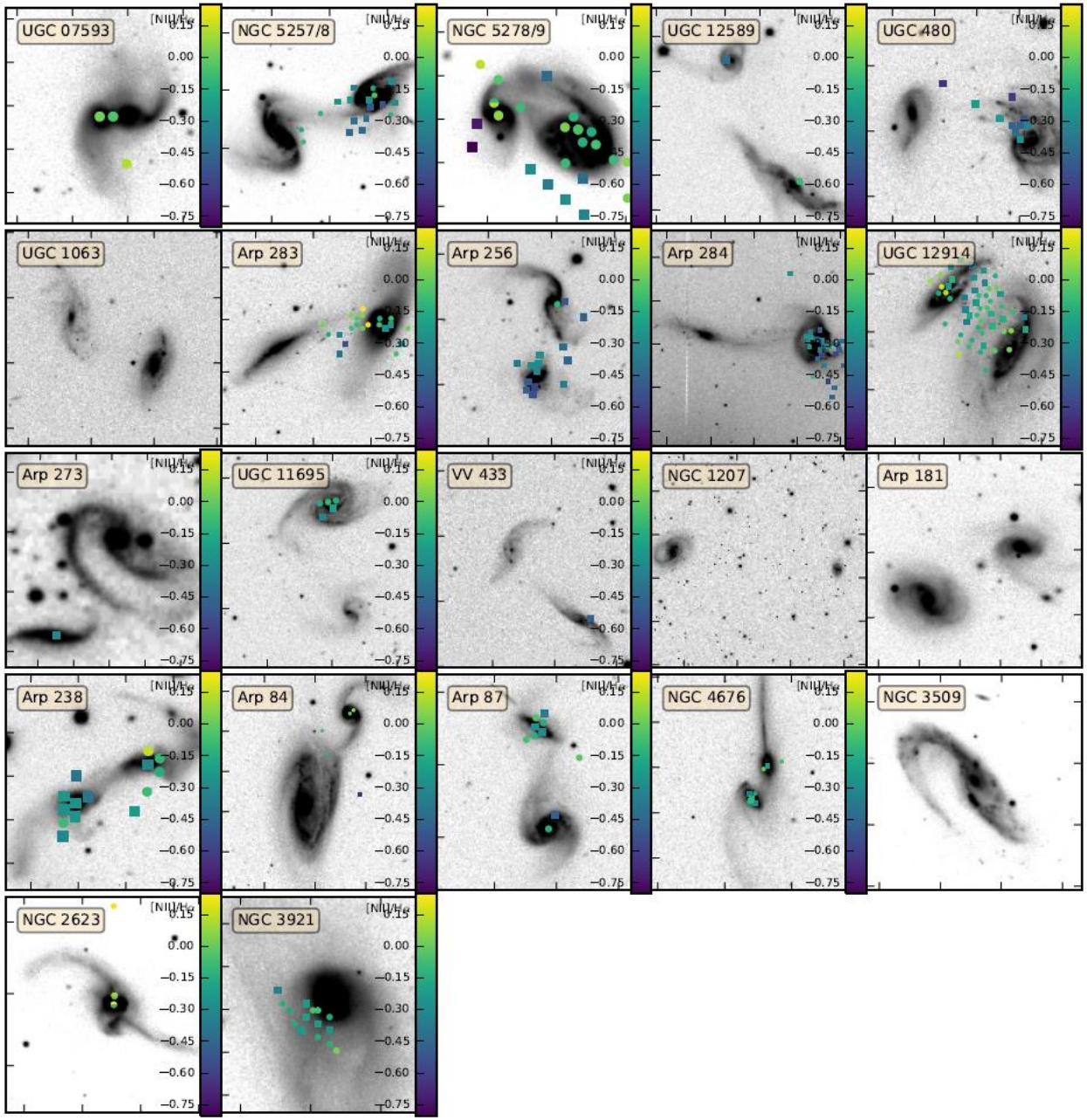

Figure 6. Collage of [N II]/Hαmaps of Group 2 and 3 components (likely to be emitted from shock-heated gas) in all of the the observed systems. Group 2 components are shown with circles and group 3 components are shown with squares. The spatial distribution of [N II]/Hα in most of the systems suggest that these components are produced by shocks.

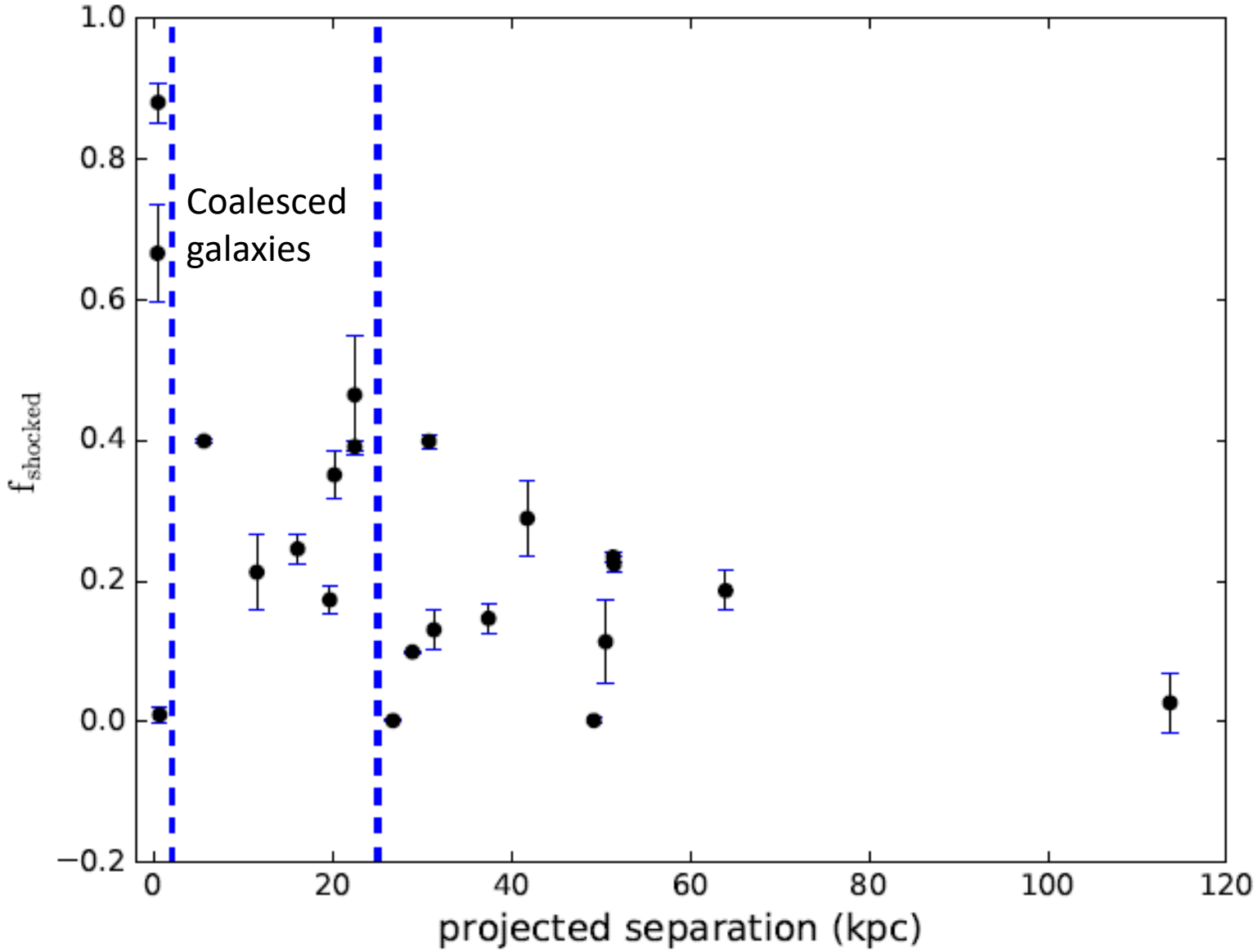
Coalesced
galaxies
1.0
0.8
0.6
0.4
0.2
0.0
−0.2
$f_{shocked}$
0
20
40
60
80
100
120
projected separation (kpc)

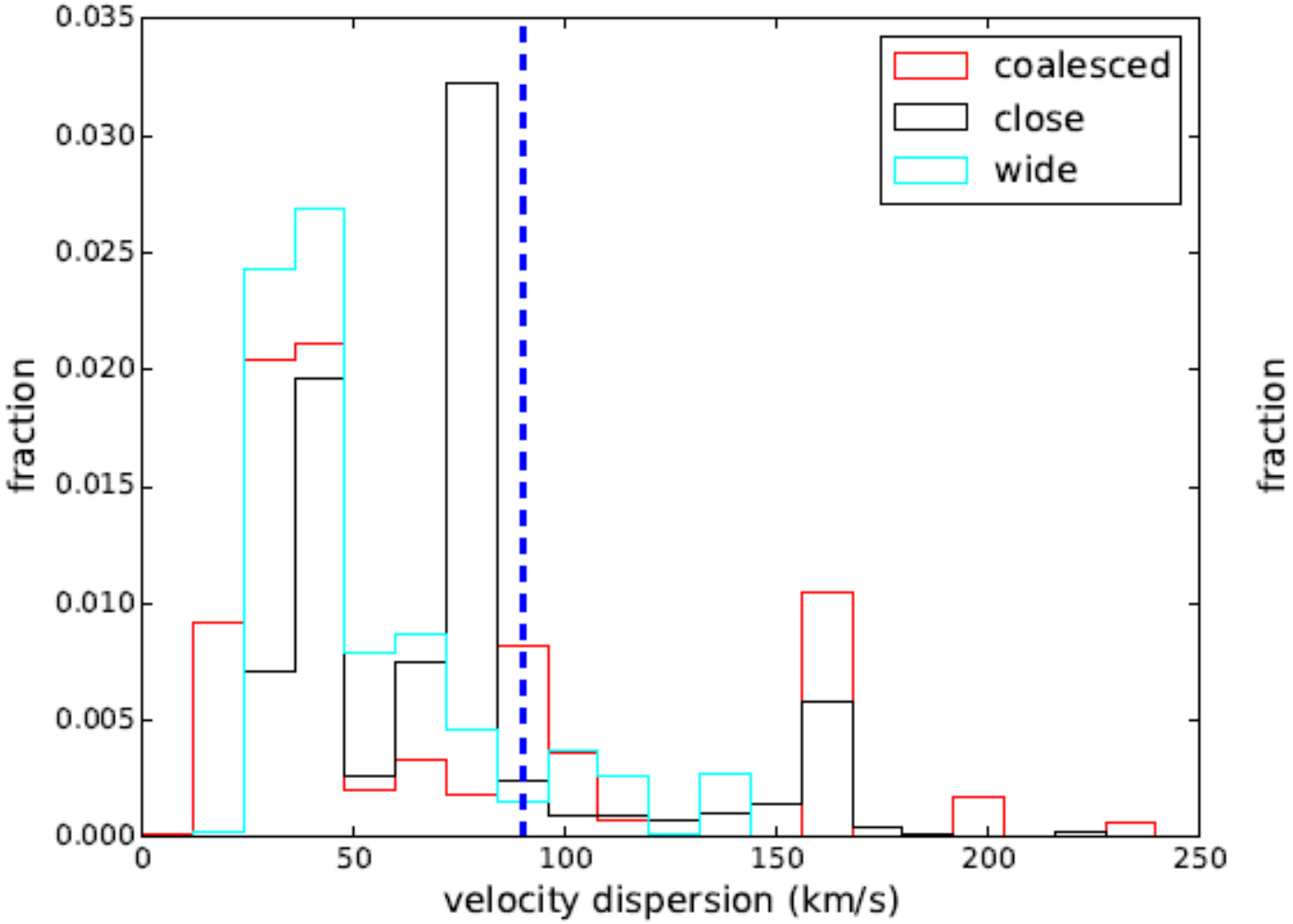
coalesced
close
wide
fraction
fraction
velocity dispersion (km/s)
0.035
0.030
0.025
0.020
0.015
0.010
0.005
0.000
0
50
100
150
200
250

Системы с динамическими моделями

system name	source	time (Myr)	Δt (Myr)	R_{peri} (kpc)	$f_{shocked}$
NGC 5257/8	Privon et al. (2013)	230.0	1200.0	21.0	0.15
NGC 4676	Mortazavi et al. (2018)	190.0	775.0	18.0	0.26
UGC 12914	Vollmer et al. (2012)	26.0	-	1.2	0.37
Arp 284	Struck & Smith (2003)	170.0	-	6.5	0.39
UGC 07593	this work	27.0	12.0	2.5	0.40
NGC 2623	Privon et al. (2013)	220.0	-80.0	1.0	0.90

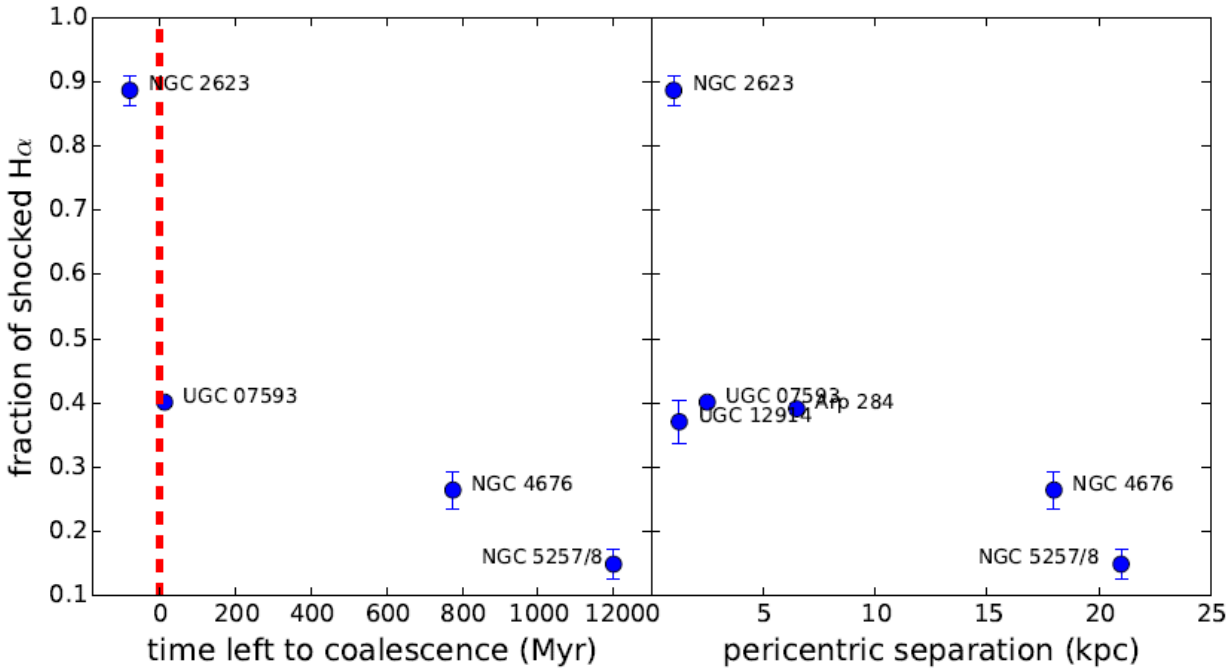

Figure 13. Trends of shock fraction in models with available dynamical model. The left panel shows how shocked Hα emission chan
with time until the galaxies coalesce in the four systems for which dynamical model provides this information. The red dashed line is
time of coalescence. The right panel shows the trend with pericentric separation.

Основные выводы

- We confirm that most of high velocity dispersion and high

[N II]/H components are galaxy wide shocks, likely to be induced as a result of interaction.

- We found that the fraction of H emission from shocked gas is correlated with the separation of galaxies in pairs. Close pairs have higher shock fraction than wide pairs.
- In the systems with dynamical models a time left to coalescence and pericentric separation appear to be correlated with the fraction of shocked Ha.
- We suggest two modes of shock production that are responsible for most of the shocks in the early stages of a merger, a) after the first passage, and b) before the coalescence.

A multiwavelength survey of HI-excess galaxies with surprisingly inefficient star formation

K. Geréb[1]⋆, S. Janowiecki[2], B. Catinella[2], L. Cortese[2], V. Kilborn[1]
[1]*Centre for Astrophysics and Supercomputing, Swinburne University of Technology, Hawthorn, VIC 3122, Australia*
[2]*ICRAR, M468, The University of Western Australia, 35 Stirling Highway, Crawley, Western Australia, 6009, Australia*

January 23, 2018

ABSTRACT

We present the results of a multiwavelength survey of H I-excess galaxies, an intriguing population with large H I reservoirs associated with little current star formation. These galaxies have stellar masses $M_\star > 10^{10}$ M$_\odot$, and were identified as outliers in the gas fraction vs. NUV$-r$ color and stellar mass surface density scaling relations based on the GALEX Arecibo SDSS Survey (GASS). We obtained H I interferometry with the GMRT, Keck optical long-slit spectroscopy and deep optical imaging (where available) for four galaxies. Our analysis reveals multiple possible reasons for the H I excess in these systems. One galaxy, AGC 10111, shows an H I disk that is counter-rotating with respect to the stellar bulge, a clear indication of external origin of the gas. Another galaxy appears to host a Malin 1-type disk, where a large specific angular momentum has to be invoked to explain the extreme $M_{\rm HI}/M_\star$ ratio of 166%. The other two galaxies have early-type morphology with very high gas fractions. The lack of merger signatures (unsettled gas, stellar shells and streams) in these systems suggests that these gas-rich disks have been built several Gyr-s ago, but it remains unclear how the gas reservoirs were assembled. Numerical simulations of large cosmological volumes are needed to gain insight into the formation of these rare and interesting systems.

Key words: Galaxies: evolution - Galaxies, radio lines: galaxies - Resolved and unresolved sources as a function of wavelength, galaxies: interactions - Galaxies

1 INTRODUCTION

Numerical simulations predict that cosmological accretion pro-

relation breaks down at low gas densities, where star-forming processes are highly inefficient. This is particularly relevant at galaxy

We are carrying out an observing campaign with the Giant Metrewave Radio Telescope (GMRT) to image the gas distribution of HI-excess galaxies.
In this paper we present the GMRT observations of four HI-excess galaxies along with VLT and Canada France Hawaii Telescope (CFHT) deep optical imaging and Keck spectroscopy.

$M_HI > 10^{10}$Msun

+выборка HI-rich gal-ex
By Brown+,2015

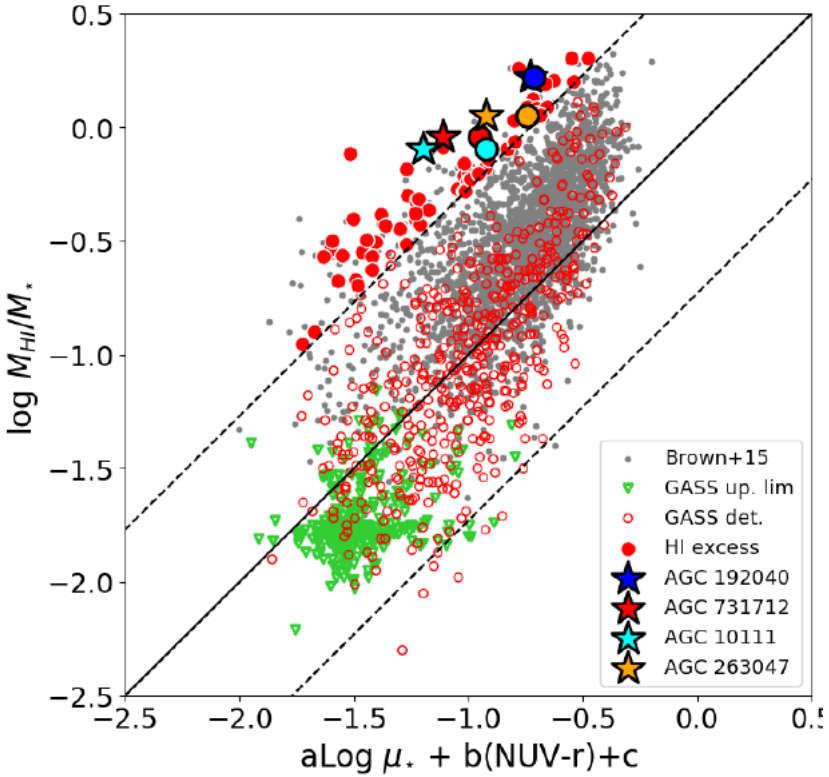

Our sample is selected from the GALEX Arecibo SDSS Survey (GASS, Catinella et al. 2010, 2013) based on the gas fraction plane, a relation between the measured H I gas fraction and that predicted from the combination of NUV−r color (a proxy for specific SFR) and stellar mass surface density ($\mu_\star$)

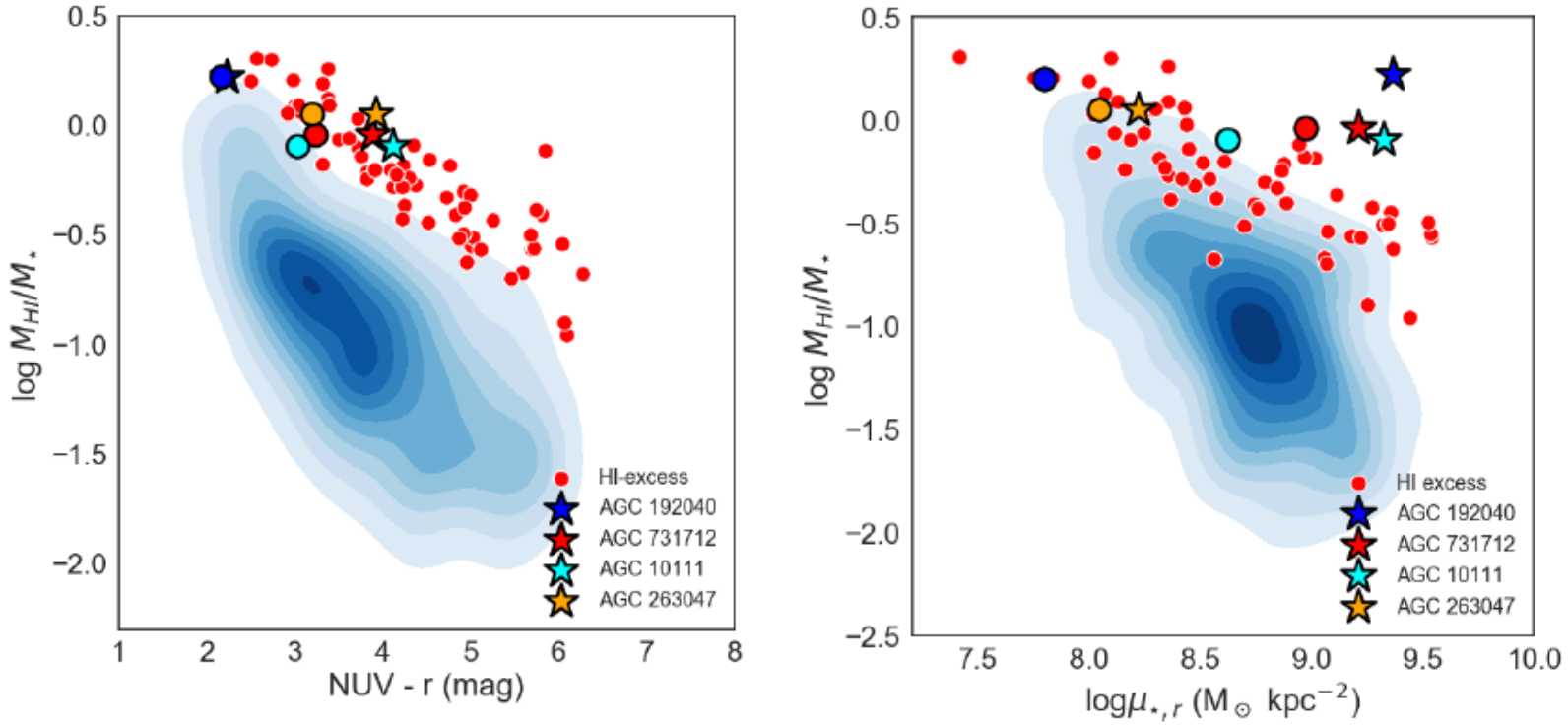

Figure 6. Left panel: H I gas fraction ($M_{\rm HI}/M_\star$) vs. NUV$-r$ colour relation of H I-excess galaxies (red points). The blue shaded region marks the GASS sample. As in Fig. 1, stars and coloured circles (revised measurements) indicate the four H I-excess galaxies discussed in this paper. Right panel: H I gas fraction vs. stellar mass surface density ($\mu_{\star,r}$) for the same samples.

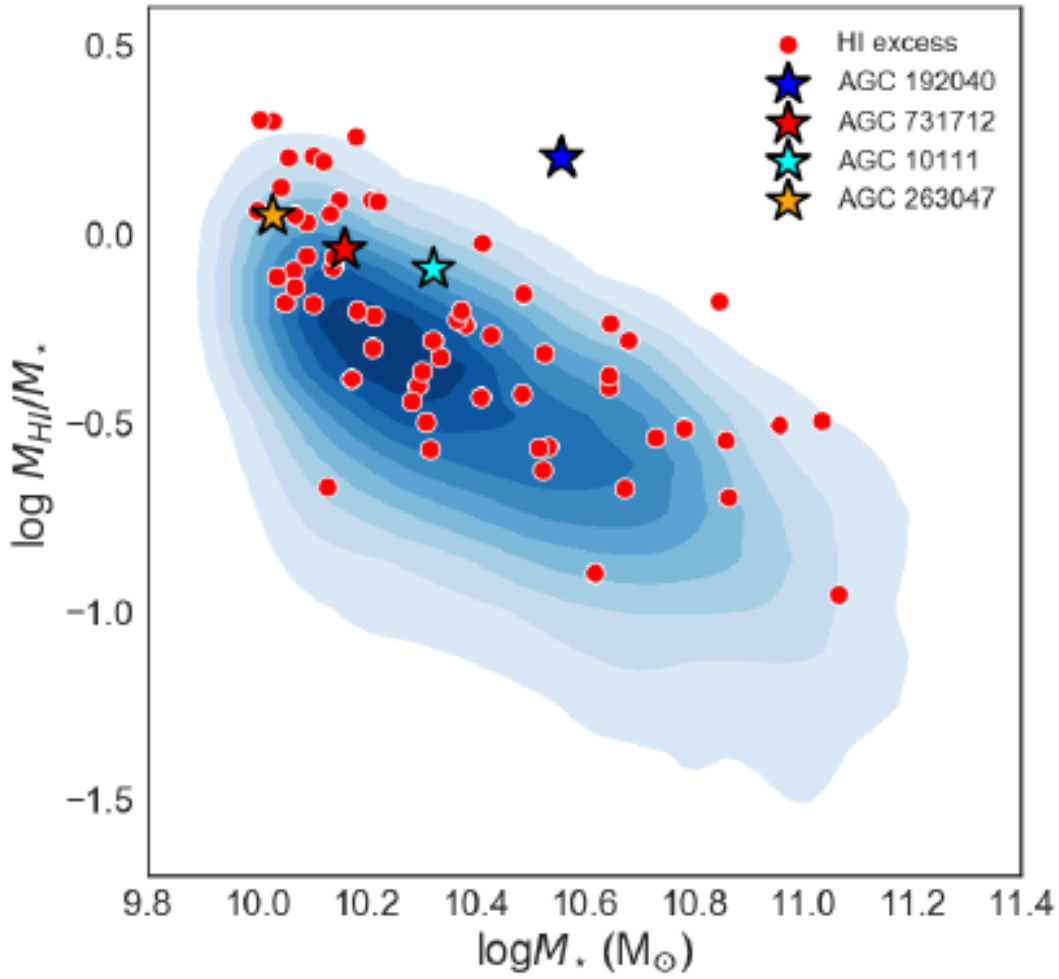

Figure 10. Gas fraction ($M_{\rm HI}/M_\star$) vs. stellar mass ($M_\star$) relation of H I-excess galaxies (red points and coloured stars), and the underlying GASS sample (blue shaded region). The $M_\star$ of AGC 192040 is based on the updated measurements.

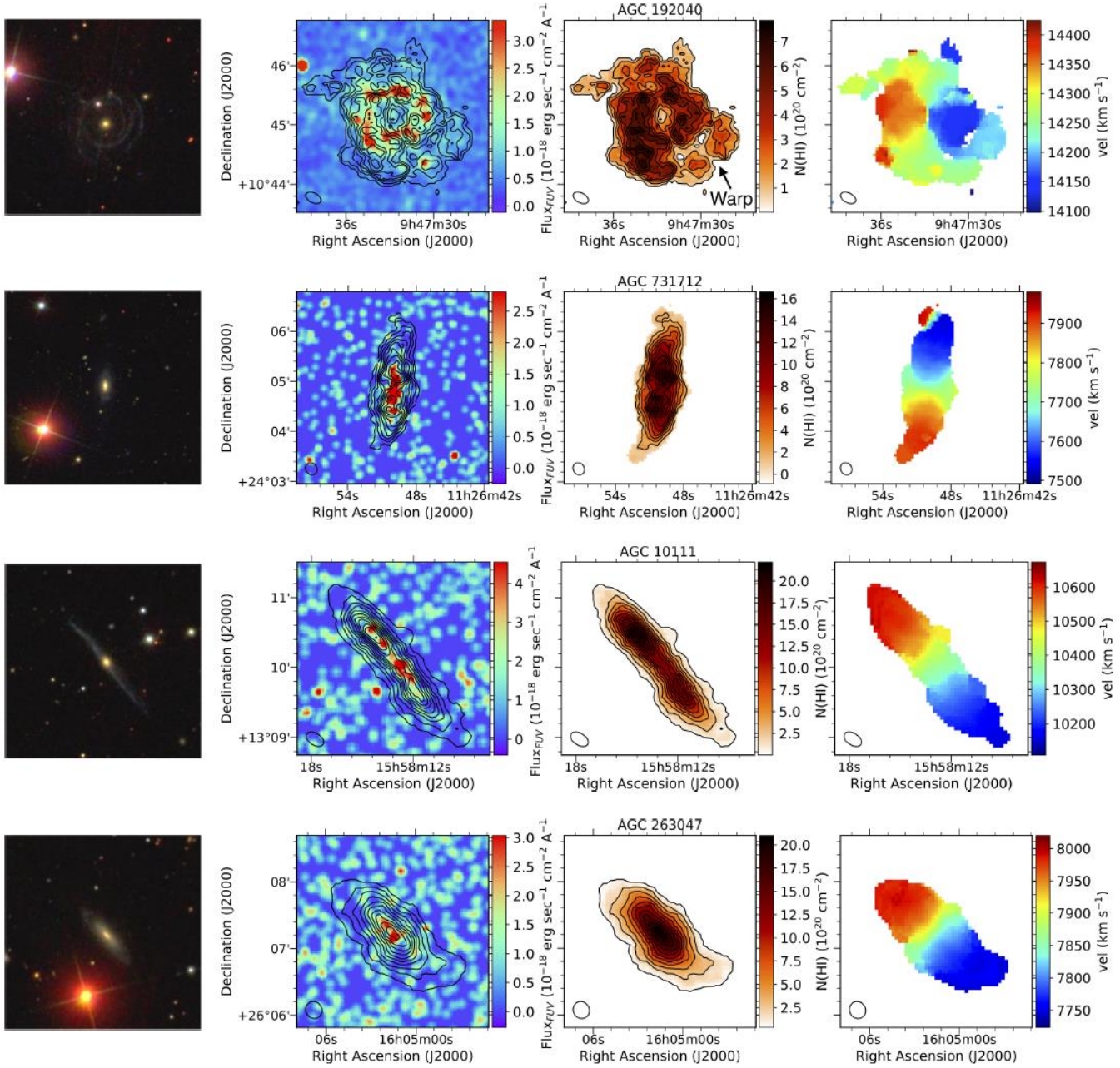

Figure 2. Multiwavelength observations of the H I-excess galaxies. From left to right: SDSS optical image, FUV image overlayed with H I contours, H I column density, H I velocity field. The SDSS images are extrated on a scale similar to the FUV and H I maps. The FUV images are smoothed by a Gaussian

Table 1. Basic properties of the H I-excess galaxies. Col.1 name used in this paper; Col.2 right ascension (J2000); Col.3 declination (J2000); Col.4 SDSS redshift; Col.5 stellar mass surface density measured from SDSS; Col.6 NUV-r color based on GALEX and SDSS measurements; Col.7; Stellar mass ; Col.8 Arecibo H I mass; Col.9 global SFR measured within the FUV radius, see Sec. 4.3 for details.

Name	RA (deg)	Dec (deg)	z	$\log\mu_\star$ ($M_\odot$ kpc^{-2})	NUV − r (mag)	$\log M_\star$ ($M_\odot$)	$\log M_{\rm HI}$ ($M_\odot$)	SFR ($M_\odot$yr^{-1})
AGC 192040	09:47:32.79	+10:45:08.72	0.0475	9.4	2.23	10.54	10.76	1.33
AGC 731712	11:26:50.06	+24:04:52.89	0.0257	9.26	3.89	10.16	10.12	0.24
AGC 10111	15:58:13.16	+13:10:07.80	0.0346	9.38	4.12	10.32	10.23	0.14
AGC 263047	16:05:01.53	+26:07:15.03	0.0263	8.44	3.92	10.03	10.08	0.05

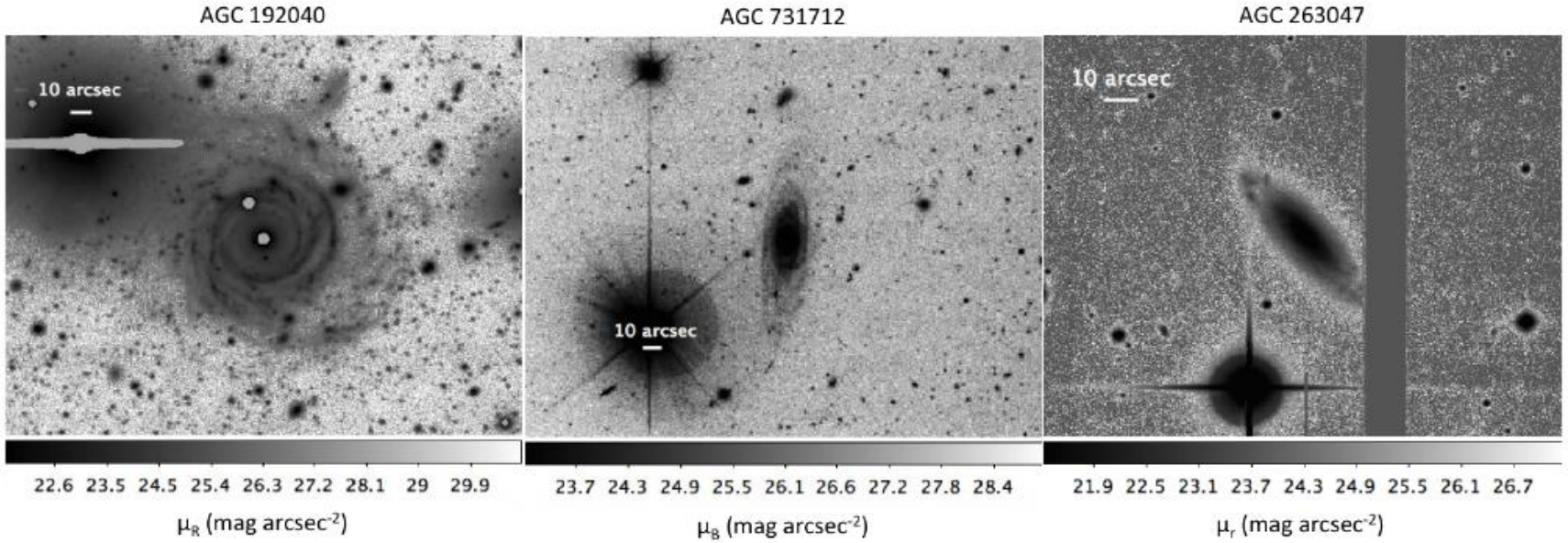

Figure 3. Deep optical images of AGC 192040 (VLT, left), AGC 731712 (CFHT, middle), and AGC 263047 (CFHT, right). The colourbars show the surface brightness (μ) in the corresponding bands.

Оптика + радио

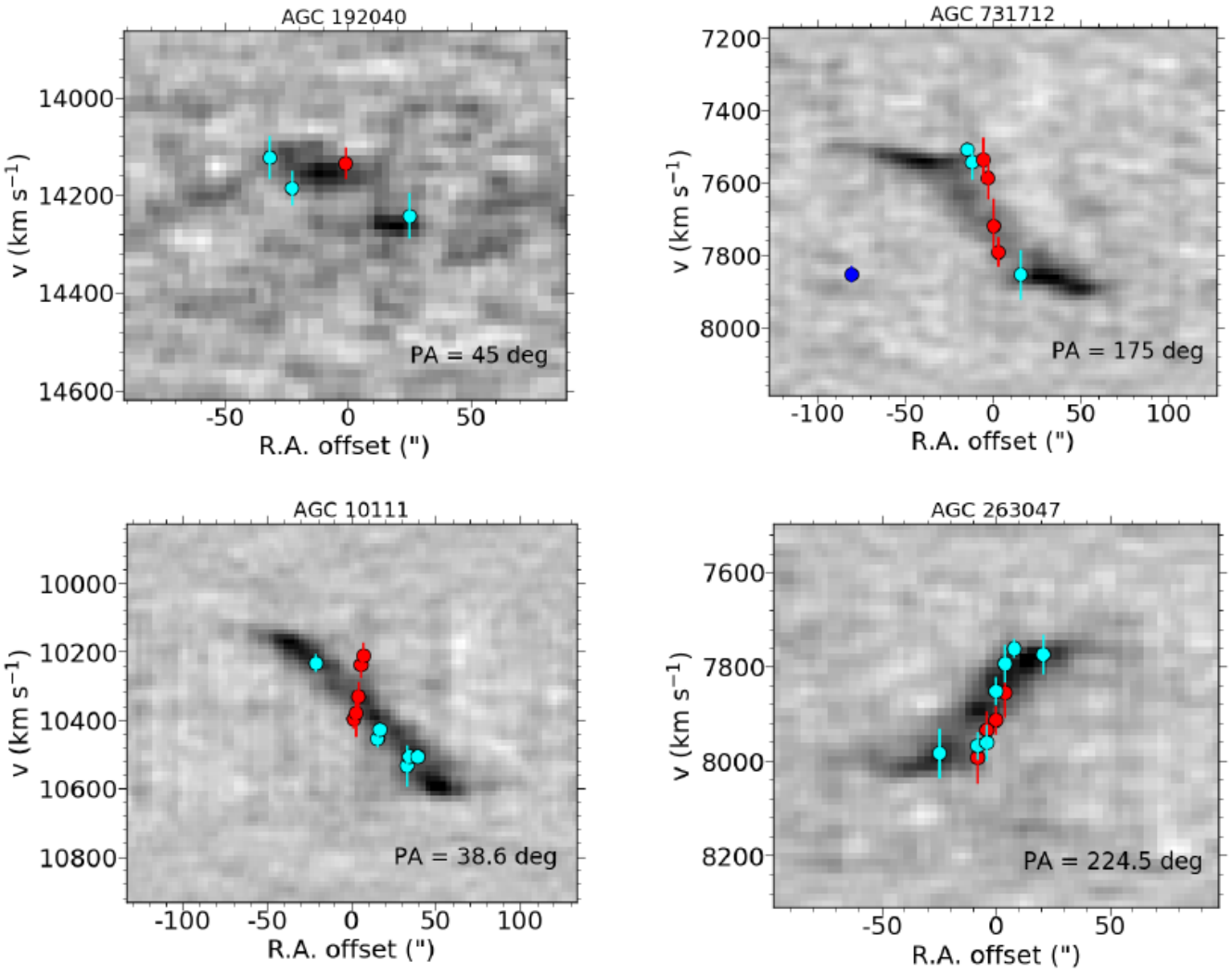

Figure 5. H I position-velocity diagrams extracted along the position angles of the Keck observations. The H I is shown by greyscales. Measurements based on the Hβ (4861.3Å), Hγ (4340.5Å), and OIII (4958.9Å, 5006.8Å) emission lines are shown as cyan points. The NaI (5892.5Å) and E-band (5269.0Å) absorption line measurements are marked in red. In the diagram of AGC 731712 (top right) the dark blue point marks the Keck detection of a dwarf galaxy. This galaxy

Основные выводы

- What HI-excess galaxies have in common is the contrast between their large gas fractions and low level of star formation, corresponding to gas depletion timescales of 10^{10} - 10^{11} year.
- AGC 192040 is a good candidate for being a Malin 1-type low surface brightness galaxy with its extended HI disk (65 kpc) and large gas fraction (logMHI /M* = 0.222), where large specific angular momentum is preserving the gas in an extended configuration.
- Counter-rotation between the gas and stars in AGC 10111 is a clear indication that the gas in this galaxy is of external origin. our detailed study indicates an external origin for the HI gas in two cases (GASS 3505 and AGC 10111), but it remains unclear how the other HI-rich systems obtained their large gas reservoirs.

THE ENIGMATIC (ALMOST) DARK GALAXY COMA P: THE ATOMIC INTERSTELLAR MEDIUM

Catherine Ball[1], John M. Cannon[1], Lukas Leisman[2], Elizabeth A.K. Adams[3,4], Martha P. Haynes[5], Gyula I.G. Józsa[6,7,8], Kristen B. W. McQuinn[9], John J. Salzer[10], Samantha Brunker[10], Riccardo Giovanelli[5], Gregory Hallenbeck[11], William Janesh[10], Steven Janowiecki[12], Michael G. Jones[13], Katherine L. Rhode[10]

[1]Department of Physics & Astronomy, Macalester College, 1600 Grand Avenue, Saint Paul, MN 55105, USA; cball@macalester.edu

[2]Department of Physics and Astronomy, Valparaiso University, Valparaiso, IN 46383

[3]ASTRON, the Netherlands Institute for Radio Astronomy, Postbus 2, 7990 AA, Dwingeloo, The Netherlands

[4]Kapteyn Astronomical Institute, University of Groningen, Postbus 800, 9700 AV Groningen, The Netherlands

[5]Center for Astrophysics and Planetary Science, Space Sciences Building, 122 Sciences Drive, Cornell University, Ithaca NY 14853 USA

[6]SKA South Africa, Radio Astronomy Research Group, 3rd Floor, The Park, Park Road, Pinelands, 7405, South Africa

[7]Rhodes University, Department of Physics and Electronics, Rhodes Centre for Radio Astronomy Techniques & Technologies, PO Box 94, Grahamstown, 6140, South Africa

[8]Argelander-Institut für Astronomie, Auf dem Hügel 71, 53121 Bonn, Germany

[9]University of Texas at Austin, McDonald Observatory, 2515 Speedway, Stop C1402, Austin, TX 78712, USA

[10]Department of Astronomy, Indiana University, 727 East Third Street, Bloomington, IN 47405, USA

[11]Washington & Jefferson College, Department of Computing and Information Studies, 60 South Lincoln Street, Washington PA 15301, USA

[12]International Centre for Radio Astronomy Research, University of Western Australia, 35 Stirling Highway, Crawley, WA 6009, Australia

[13]Instituto de Astrofísica de Andalucía, Glorieta de la Astronoma s/n, 18008 Granada, Spain

Abstract

We present new high-resolution HI spectral line imaging of Coma P, the brightest HI source in the system HI 1232+20. This galaxy with extremely low surface brightness was first identified in the ALFALFA survey as an "(Almost) Dark" object: a clearly extragalactic HI source with no obvious optical counterpart in existing optical survey data (although faint ultraviolet emission was detected in archival GALEX imaging). Using a combination of data from the Westerbork Synthesis Radio Telescope and the Karl G. Jansky Very Large Array, we investigate the HI morphology and kinematics at a variety of physical scales. The HI morphology is irregular, reaching only moderate maxima in mass surface density (peak $\sigma_{\rm HI} \sim 10$ M$_\odot$ pc^{-2}). Gas of lower surface brightness extends to large radial distances, with the HI diameter measured at 4.0±0.2 kpc inside the 1 M$_\odot$ pc^{-2} level. We quantify the relationships between HI gas mass surface density and star formation on timescales of ∼100-200 Myr as traced by GALEX far ultraviolet emission. While Coma P has regions of dense HI gas reaching the $N_{\rm HI} = 10^{21}$ cm^{-2} level typically associated with ongoing star formation, it lacks massive star formation as traced by Hα emission. The HI kinematics are extremely complex: a simple model of a rotating disk cannot describe the HI gas in Coma P. Using spatially resolved position-velocity analysis

Coma-P

- Extremely LSB. Найдена по ALFALFA blind HI extragalactic survey. no obvious
- No optical counterpart in existing optical survey data (although faint ultraviolet emission was detected in archival GALEX imaging).
- Subsequent detailed HI and optical follow-up observations presented in Janowiecki et al. (2015) revealed a stellar population of extremely low surface brightness stellar population with extended HI gas. This source, AGC 229385, we hereafter will refer to as Coma P."

WIYN 3.5m

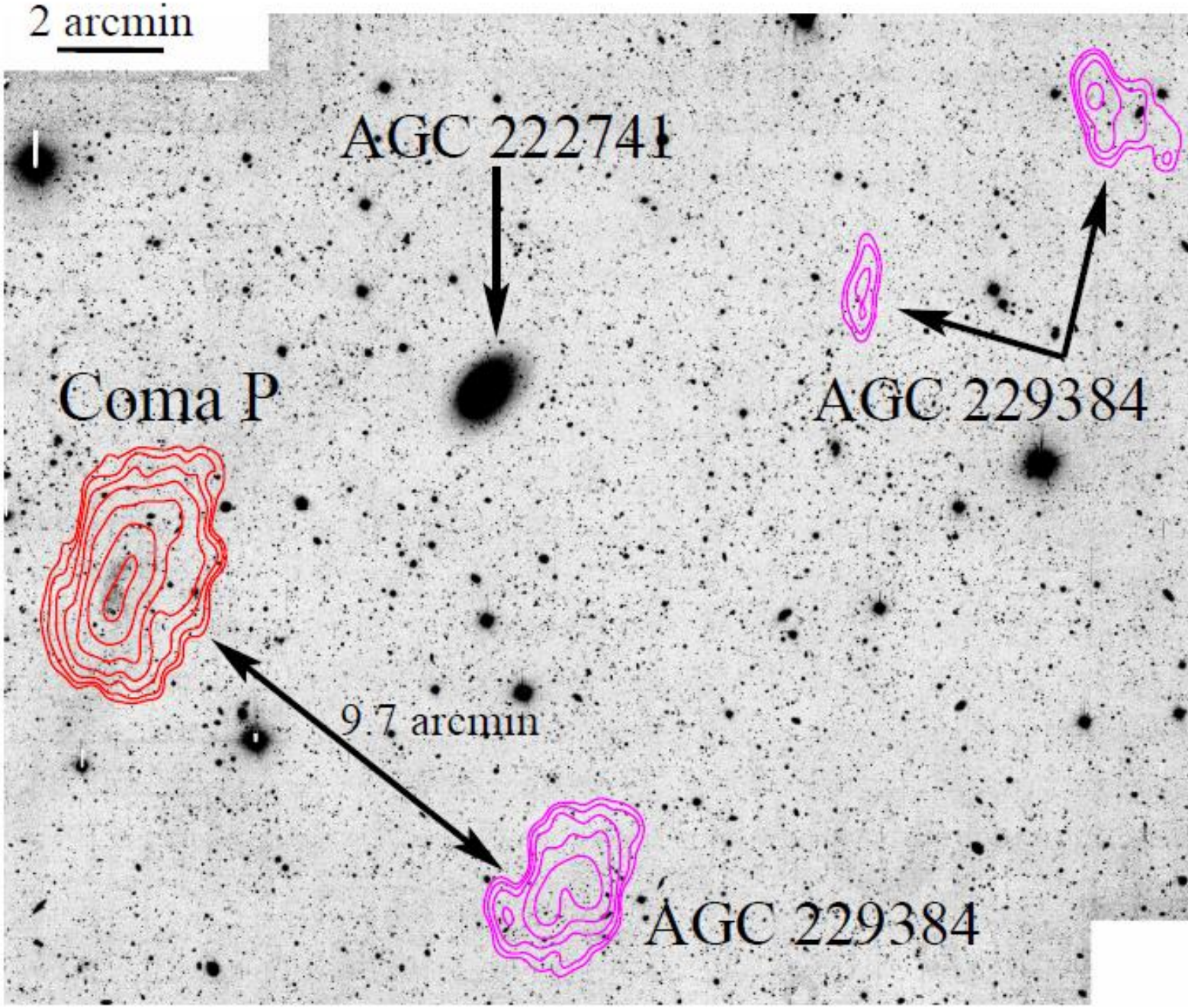

- In this work, we present new HI line synthesis observations of the neutral interstellar medium of ComaP constructed by combining new higher resolution Very Large Array (VLA4) HI line imaging with the WSRT HI line dataset.

HST

- Peak surface brightnesses

in the g’, r’, and I’ bands are
26.4 mag arcsec^2,
26.5 mag arcse^2, and
26.1 mag arcsec□ 2, respectively

All of the stellar population of ComaP is located within HI gas with NHI > 510^20 cm^2 (4.0 M pc^2).

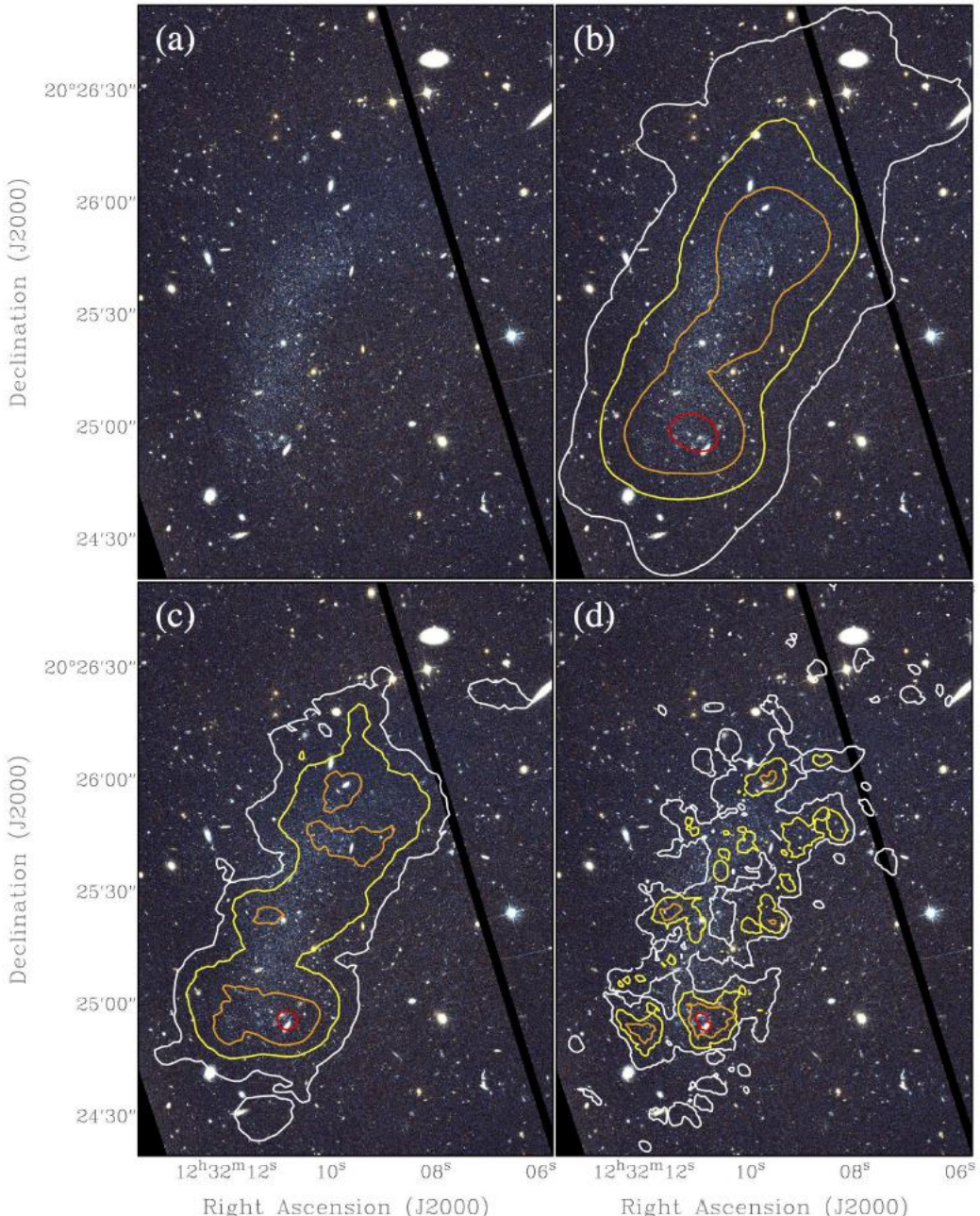

Table 1. Physical Characteristics of Coma P

Parameter	Value
R.A. (J2000)	$12^{h}\ 32^{m}\ 10^{s}.3$
Decl. (J2000)	$+20°25'23''$
Adopted distance (Mpc)	5.50 ± 0.28^{a}
M_B (mag)	-10.71 ± 0.14^{a}
$M_\star$ ($M_\odot$)	$(1.0 \pm 0.3) \times 10^{6a}$
M_{HI} ($M_\odot$)	$(3.48 \pm 0.35) \times 10^{7b}$
D_{HI} (kpc)^{c}	4.0 ± 0.2
SFR_{FUV} ($M_\odot\,yr^{-1}$)	$(3.1 \pm 1.8) \times 10^{-4}$

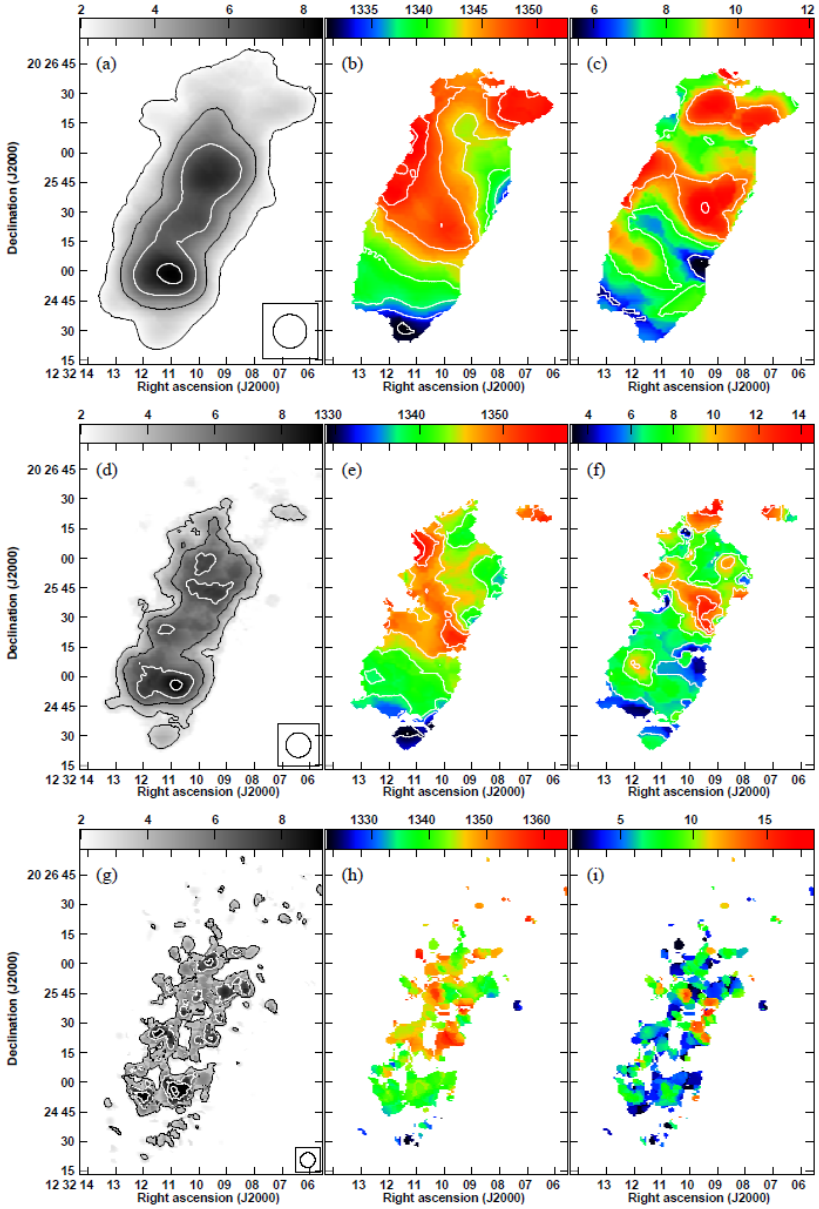

Figure 6. HI images of Coma P at low (top row, 17″ beam), medium (middle row, 12.″5 beam), and high (bottom row, 7.″5 beam) resolution. Panels (a), (d), and (g) show HI column density in units of 10^{20} cm^{-2}. Contours are overlaid at levels of $(2,4,6,8) \times 10^{20}$ cm^{-2}, $(3,5,7,9) \times 10^{20}$ cm^{-2}, and $(3,6,9,12) \times 10^{20}$ cm^{-2} in panels (a), (d), and (g), respectively. Panels (b), (e), and (h) show the intensity-weighted HI velocity field in units of km s^{-1}. The contours in panel (b) span the range of 1331–1352 km s^{-1} in intervals of 3 km s^{-1}, while the contours in panel (e) span the range of 1330–1354 km s^{-1}in intervals of 4 km s^{-1}. Panels (c), (f), and (i) show the intensity-weighted HI velocity dispersion in units of km s^{-1}: the contours in panels (c) and (f) are at levels of (6,8,10,12) km s^{-1}. No contours are shown in panels (h) and (i) for ease of interpretation.

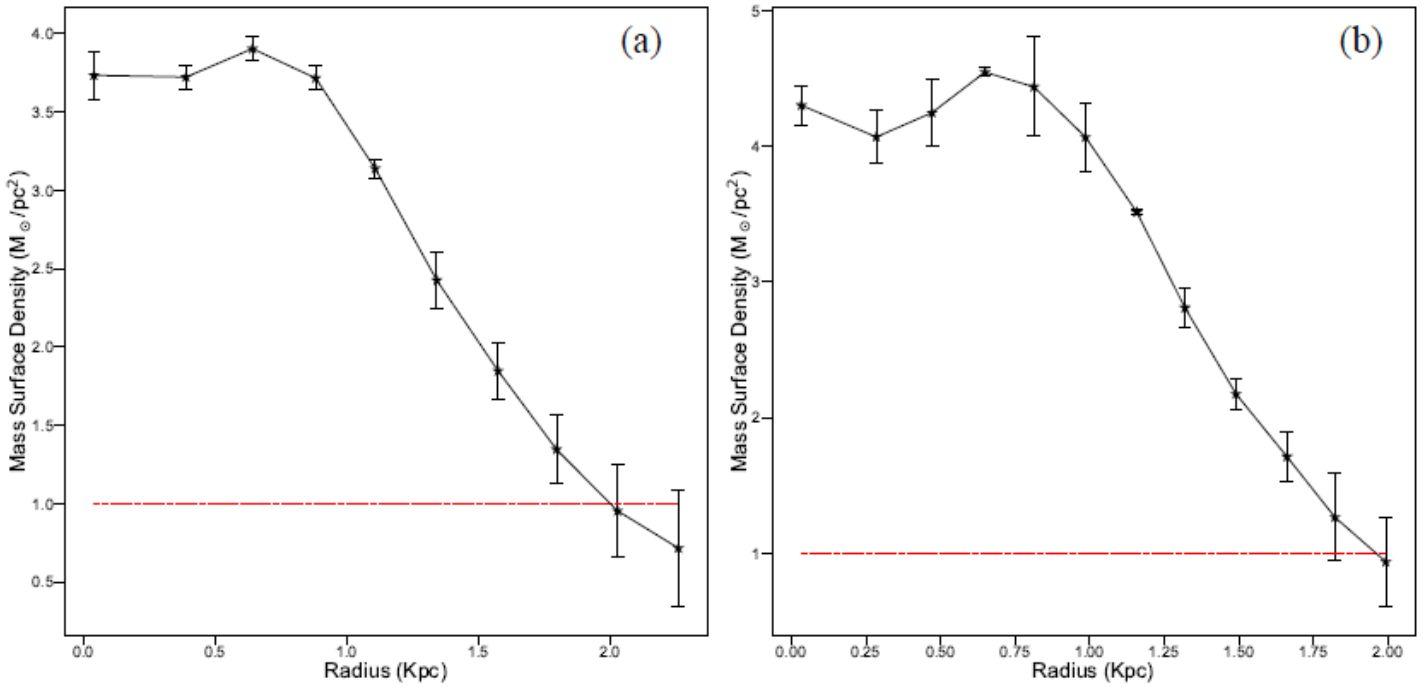

Figure 7. Radially integrated profiles of HI mass surface density as a function of radial distance from the adopted morphological center of the galaxy $(\alpha,\delta) = (12^{\rm h}32^{\rm m}10.^{\rm s}3,\ +20^\circ25'23'')$ using (a) the low-resolution (17″ beam or 453 pc physical resolution) and (b) the medium resolution (12.″5 beam or 333 pc physical resolution) HI data. These profiles have been corrected for inclination ($i = 63^\circ$) and for beam smearing as described in Wang et al. (2016). The dotted red line denotes a mass surface density of 1 $M_\odot\,pc^{-2}$. The HI diameter of Coma P is 4.0 ± 0.2 kpc.

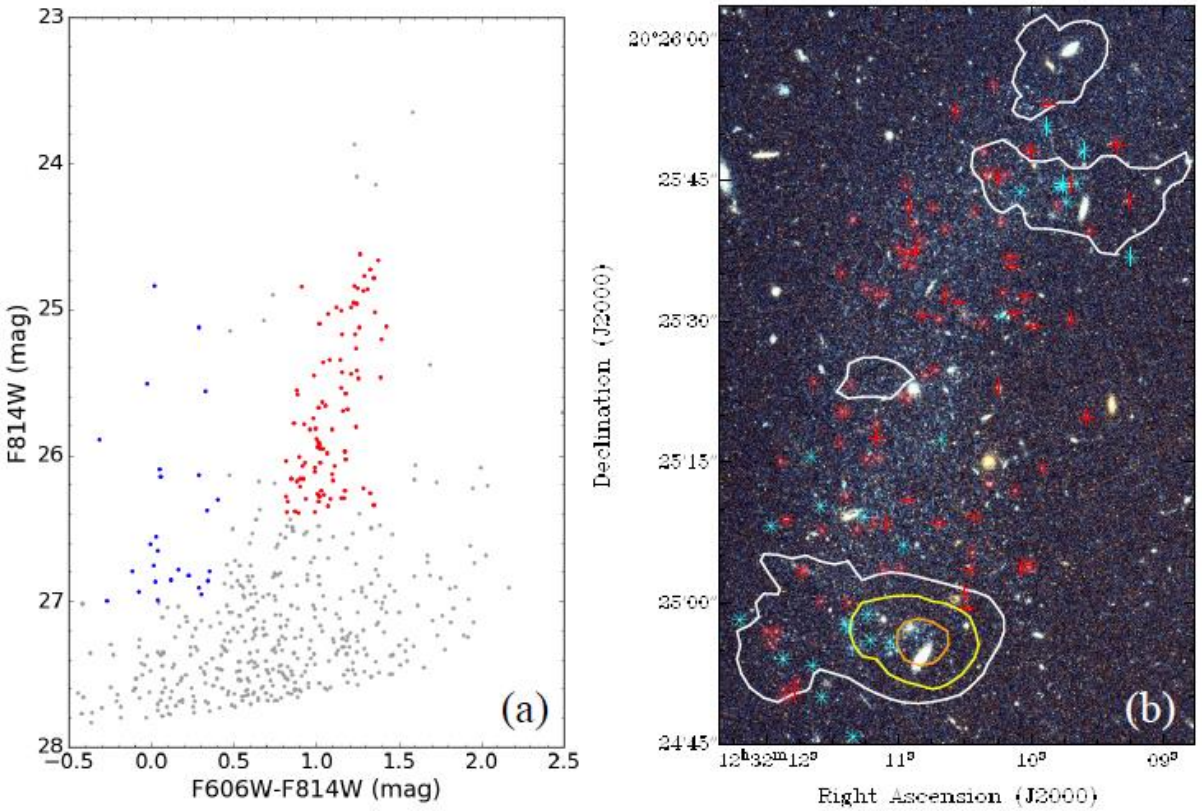

Figure 9. The locations of red and blue stars in Coma P. Panel (a) shows the color-magnitude diagram as presented in Brunker et al. (2017, in preparation). Selected red and blue stars are color-coded (see detailed discussion in § 4). These stars are plotted as cyan (representing blue stars) and red (representing red stars) asterisks in panel (b). The color HST image is slightly enlarged compared to the field shown in Figure 8. HI column density contours from the medium-resolution (12.″5 beam) data are overlaid: white, yellow, and orange encode HI column densities of $(7,\ 8,\ 9) \times 10^{20}$ cm^{-2}, respectively. The red stars are uniformly distributed throughout the galaxy, while the blue stars are strongly concentrated in the regions of highest HI mass surface density.

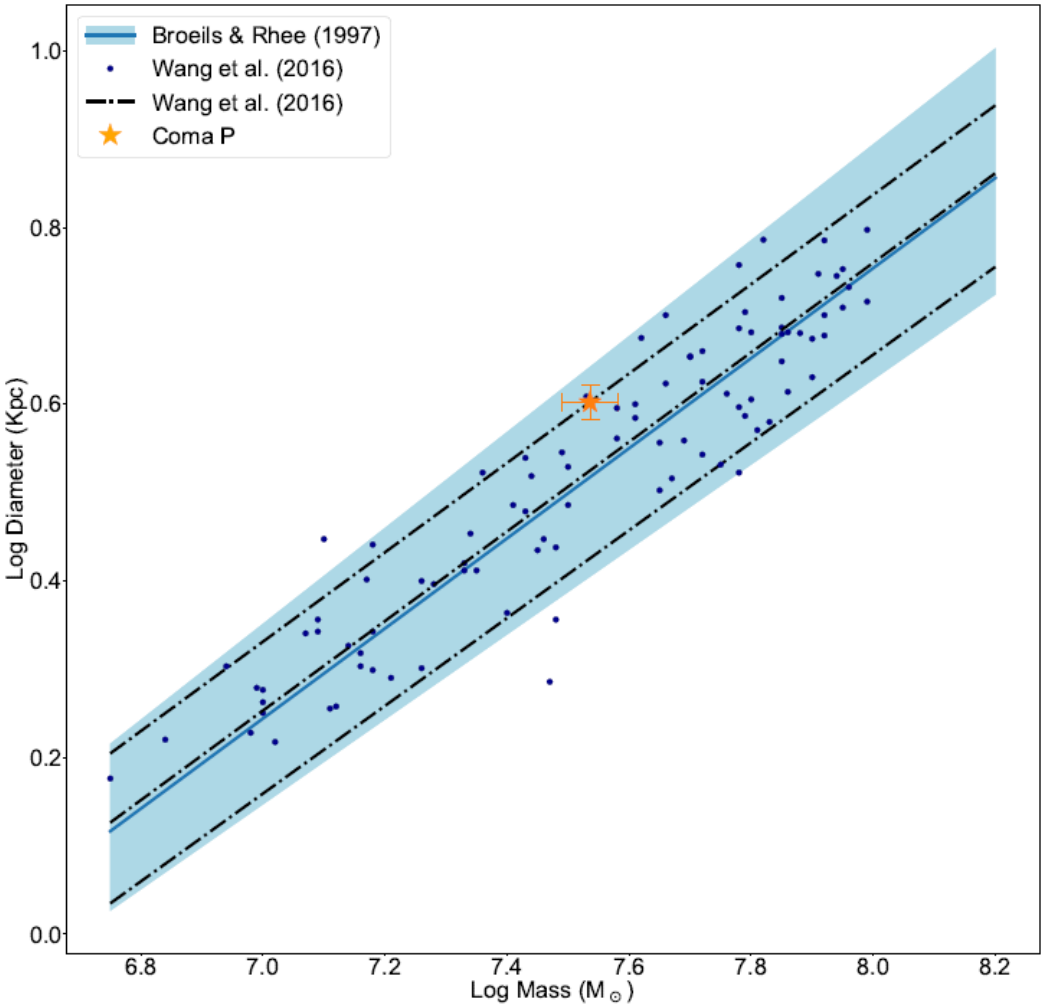

Figure 16. The M_{HI} – D_{HI} relation, showing Coma P and a subset of the comparison galaxies from Wang et al. (2016). The HI diameters of all galaxies are determined at the 1 $M_\odot\,pc^{-2}$ level. The dash–dot lines show the best-fit relation and the 3σ scatter from Broeils & Rhee (1997). The solid line shows the best-fit relation from Wang et al. (2016), and the shaded blue region shows the 3σ scatter. The slopes of the M_{HI} – D_{HI} relation as derived by Broeils & Rhee (1997) and Wang et al. (2016) are effectively identical. Coma P is just consistent with the 3σ scatter of the relation of Wang et al. (2016). This galaxy can be considered to have a large HI diameter given its HI mass or a low HI mass given its physical size.

Using the most obvious signatures of rotation in the three-dimensional data, we estimate the total dynamical mass of the ComaP system to be (1 .2\pm0.6)10^8 M. It is important to note that this is the sum of the estimates of the dynamical masses of the two kinematically distinct HI components. ComaP is not unusually dominated by dark matter (Mdyn/Mbary ~2.5) compared to other Local Volume dwarf galaxies with similar dynamical masses.

Regardless of their origins, the physical characteristics of ComaP make it an exceptional galaxy. Its physical properties are among the most extreme of any known source in the Local Volume. ComaP will serve as a critical benchmark for our understanding of low-mass galaxy evolution.